Physica Medica 65 (2019) 106–113

Contents lists available at ScienceDirect

Physica Medica

journal homepage: www.elsevier.com/locate/ejmp

Original paper

High resolution radiochromic film dosimetry: Comparison of a microdensitometer and an optical microscope

P. Pellicioli[a,b,c,*], S. Bartzsch[d,e], M. Donzelli[a,f], M. Krisch[a], E. Bräuer-Krisch[a,1]

[a] The European Synchrotron Radiation Facility, ID17 Biomedical Beamline, Grenoble, France
[b] Inserm UA7 STROBE, Grenoble Alpes University, Grenoble, France
[c] Swansea University Medical School, Singleton Park, Swansea SA2 8PP, United Kingdom
[d] Helmholtz-Centre Munich, Institute of Innovative Radiation Therapy, Munich, Germany
[e] Klinikum rechts der Isar, Department for Radiation Oncology, Technical University of Munich, Germany
[f] ICR – The Institute of Cancer Research, London, United Kingdom

ARTICLE INFO

Keywords:
Microbeam radiation therapy
Radiochromic film dosimetry
Microdensitometer
Optical microscope

ABSTRACT

Purpose: Microbeam radiation therapy is a developing technique that promises superior tumour control and better normal tissue tolerance using spatially fractionated X-ray beams only tens of micrometres wide.

Radiochromic film dosimetry at micrometric scale was performed using a microdensitometer, but this instrument presents limitations in accuracy and precision, therefore the use of a microscope is suggested as alternative. The detailed procedures developed to use the two devices are reported allowing a comparison.

Methods: Films were irradiated with single microbeams and with arrays of 50 μm wide microbeams spaced by a 400 μm pitch, using a polychromatic beam with mean energy of 100 keV. The film dose measurements were performed using two independent instruments: a microdensitometer (MDM) and an optical microscope (OM).

Results: The mean values of the absolute dose measured with the two instruments differ by less than 5% but the OM provides reproducibility with a standard deviation of 1.2% compared to up to 7% for the MDM. The resolution of the OM was determined to be ~ 1 to 2 μm in both planar directions able to resolve pencil beams irradiation, while the MDM reaches at the best 20 μm resolution along scanning direction. The uncertainties related to the data acquisition are 2.5–3% for the OM and 9–15% for the MDM.

Conclusion: The comparison between the two devices validates that the OM provides equivalent results to the MDM with better precision, reproducibility and resolution. In addition, the possibility to study dose distributions in two-dimensions over wider areas definitely sanctions the OM as substitute of the MDM.

1. Introduction

Microbeam Radiation Therapy (MRT) is a recent pre-clinical technique that promises to be more effective than conventional radiotherapy techniques (RT) in tumour treatment [1–3] with fewer biological side effects [4,5]. Pre-clinical studies suggest that MRT may be extremely useful to treat certain pathologies such as brain gliomas in paediatric patients, where the surrounding healthy tissue is particularly sensitive to radiation [6].

The main feature of MRT is the use of arrays of quasi-parallel microbeams, typically 50 μm wide beams spaced by 400 μm pitch, with hundreds of gray (Gy) in the peak and a low dose between the beams further referred to as valley dose. In addition, medium-energy X-ray photons (mean energy around 100 keV) are used instead of MeV photons to reduce the travel range of secondary electrons in the tissues, and the divergence of the beam must be small to preserve the microbeams shape throughout the target. The extremely high dose rates achievable with synchrotron X-rays [7–9] allow reducing the exposure time and avoiding the blur of the microbeams traces due to tissue motion that in the human brain has a motion range up to hundreds of micrometres with a maximum motion velocity of 2 mm/s [10–12].

MRT is currently best performed at a third generation synchrotron where microbeams are generated by a high brilliance X-ray source [1] able to satisfy the beam characteristics described above. All the experiments performed and reported in this paper were performed in Grenoble, France, at the biomedical beamline ID17 of the ESRF – the

* Corresponding author at: The European Synchrotron Radiation Facility, ID17 Biomedical Beamline, 71 avenue des Martyrs, CS 40220, 38043 Grenoble Cedex 9, France.
E-mail address: paolo.pellicioli@esrf.fr (P. Pellicioli).
[1] Deceased September 10, 2018.

https://doi.org/10.1016/j.ejmp.2019.08.012
Received 22 April 2019; Received in revised form 13 August 2019; Accepted 14 August 2019
Available online 23 August 2019

European Synchrotron – where the X-ray source is placed at around 40 m distance from the target [13] and allows the generation of quasi-parallel microbeams at a dose rate of around 14 kGy/s.

Until now, absolute dosimetry at micrometric scale has been a challenge in MRT because the irradiation parameters involved are extreme compared to classical approaches. The high dose rate of the source can cause detector saturation; the resolution on a micrometric scale at the target position is necessary to resolve the dose distribution of the microbeams; the materials used in the realization of the detector should be tissue equivalent around 100 keV photon energy. Potential high resolution detectors and dosimeters such as silicon strip, MOSFET, TLD and others have been designed and tested since the beginning of the development of MRT [14], however a final and definitive solution is not yet established because none of these devices is able to satisfy and achieve all the requirements in MRT. Detector developments are therefore still an active R&D area [15].

Between the most recent works on detectors applied for MRT studies, PRESAGE® dosimetry plastics are able to visualize the delivered dose in a 3D volume [16] but the combination of the spatial resolution of the material with the optical computed tomography system used for the analysis still does not allow to properly resolve the peak dose of the microbeams [17]. Silicon strip detectors constantly evolved since their first realization and their sensitive volume was recently decreased to a thickness of 5 μm when used in passive mode [18]. The PTW microDiamond™ detector (PTW-Freiburg GmbH, Freiburg, Germany) has a nominal circular active volume of 1.1 mm radius and 1 μm thickness able to resolve the microbeam dose distribution if scanned perpendicular to the microbeam extension [19]. These electronic dosimeters allow punctual dose measurements in real time, but their geometry requires a precise and time-consuming alignment procedure if a micrometric dose resolution is desired and they are not suitable for delivering dose maps in a reasonable amount of time. In the last years, the use of fibre-optical dosimeters for the dose evaluation in MRT was tested [20] as well, and only recently a 20 μm dose resolution was achieved opening the possibility of microbeams characterization [21].

The current study focuses on the use of radiochromic films to evaluate doses on a micrometre scale. Radiochromic films are already used for dose evaluation in conventional RT for relative dosimetry and quality assurance [22,23], and they are a promising detector candidate for MRT with the ability to detect 2-dimensional dose maps with less than 5 μm spatial resolution. Films do not allow real-time dosimetry, but they are relatively easy to handle and used for dose measurement in plastic phantoms [24].

Until recently, the read-out of the films irradiated with microbeams was performed using microdensitometers [13,25] but a new way involving optical microscopes was suggested for the analysis of the radiochromic film [26,27] to overcome the limitations in accuracy, precision and time consumption in the use of the microdensitometers. The nominal specifications of a recent optical microscope easily surpass the specification of a microdensitometer but an actual film read-out comparison between the two instruments and their protocols for the read-out operation was never performed. As first step in the acceptance of the most recent protocol, it is fundamental to verify that the use of the microscope can effectively be considered a valid implementation for film dosimetry without introducing measurement differences.

The aim of this study is to compare a Joyce Loebl 3CS microdensitometer (MDM) and an inverted Zeiss Axio Vert.A1 optical microscope (OM) in terms of accuracy, reproducibility, stability and versatility for the analysis of radiochromic film on a micrometric scale. The comparison of the dose values obtained from the same set of irradiated films using the two devices will be presented to verify the absence of major differences in film dosimetry for MRT. Focus will be placed on the description of the most recent and updated protocols developed for both instruments, explaining how the same read-out approach must be adapted at the devices' limits and characteristics. The OM will be proven to be superior in reliability with a less time-consuming read-out procedure. Furthermore, profiting from the much higher spatial resolution of the OM in both spatial directions, we analysed films irradiated with the pencil beam configuration. Pencil beam irradiation is based on a beam cross section of only $50 \times 50\ \mu m^2$ and dose evaluation is even more challenging compared to microbeams because the spatial fractionation is present in two directions. This level of analysis cannot be performed with other detectors tested in MRT while it can be reached using radiochromic film dosimetry.

2. Materials

2.1. Radiochromic films

Gafchromic® is a brand of radiochromic films developed by Ashland industries, designed for quantitative measurements of absorbed radiation dose. The Gafchromic® HD-V2 series [28] was used in this study because its dynamic dose range is between 10 and 1000 Gy and matches the dose delivered in MRT. The HD-V2 film is composed of only two layers: an active layer nominally 12 μm thick and a polyester substrate nominally 97 μm thick. The active material includes the diacetylene monomer, a radio-sensitive active monomer that polymerises after irradiation and causes a colour/opacity change [29,30] related to the dose delivered.

One important feature of Gafchromic® films is their near tissue equivalence [30]. Moreover, they do not require post-exposure chemical treatment. However, it was observed that they need about 24 h after irradiation until the optical density stabilises [31]. Under these conditions, real-time dose measurements are not possible, and the read-out of the film is done 1–4 days after the exposure. Studies on the granularity of the materials used in the film fabrication demonstrate that the resolution of this HD-V2 detector is about 2 μm to 3 μm [27], sufficient to sample the 50 μm wide beams used.

2.2. Microdensitometer

Until recently, the analysis of MRT irradiated films was only performed using a microdensitometer (MDM) such as the Joyce Loebl Automation Ltd 3CS available at the ESRF. This instrument was designed for the measurement of optical densities through a true double-beam light system, where two light beams from a halogen source are split into two different paths: one passes through the film while the second is attenuated by an optical wedge of known density. A photomultiplier receives alternately the two beams and the output signal produced by the amplifier is sent to the motor connected to the wedge. If an intensity difference between the two beams is present, the motor moves the wedge and equalises the intensity such that the position of the wedge corresponds to the optical density of the sample.

For the analysis, the film is loaded on a mechanical platform that can be moved along the plane in steps of 1.2 μm. Under standard working conditions, the horizontal resolution (perpendicular to the microbeams and along the scanning direction) is between 20 μm and 25 μm [25,32], calculated from the modulation transfer function (MTF). The resolution parallel to the microbeams is defined by the minimum iris dimension of the MDM optics and it cannot be reduced below 2 mm due to mechanical restrictions.

2.3. Optical microscope

Since 2013, an inverted Zeiss Axio Vert.A1 optical microscope is installed at the ESRF for film read out. It is equipped with a light-emitting diode (LED) source (wavelength range from 400 nm to 700 nm) and a motorised scanning stage that controls the position with a precision of 0.1 μm. A tunable condenser aperture determines the depth of focus which can be adjusted between 2 μm and 45 μm. The aperture dimension influences also the light intensity on the specimen but the image brightness can be regulated by changing the LED voltage

or the exposure time of the charge-coupled device (CCD) camera.

A Zeiss AxioCam MRm camera [33] is mounted to acquire images with 12-bit grey level using a CCD with a basic resolution of 1388 × 1040 and a pixel size of 6.45 μm in both directions. The Zeiss EC Plan-Neofluar objectives are mounted with magnification/numerical aperture of 5x/0.16 to obtain a nominal resolution for each image pixel of 1.29 μm on the film surface. With this setup, the objective provides a field of view of 1.79 × 1.34 mm^2 but a wide film area can be obtained by using the Zeiss mosaiX software that is able to coordinate the motorized scanning stage movement with the camera acquisition and stitch images together to increase the final field of view. The optical resolution of the OM was measured by the MTF normalized to the value at zero frequency and it is 0.1 at ~ 330 line pairs per millimeter, corresponding to a spatial resolution of 1.52 μm.

3. Methods

3.1. Film preparation and irradiation

In this work, the largest field used was 3 × 3 cm^2 therefore a single sheet of Gafchromic® film was cut into several pieces avoiding the possible variation in sensitivity response between sheets. To reduce the structural defects due to the cut, a 5 mm wide border of non-irradiated film was left on the margin of the field edges. Due to the manufacturing process, variations in the film sensitivity are higher along the short edge of the film sheet [34]. For this reason, the set of film for calibration and measurements was always taken from the same column as defined by the long sheet edge of the same film sheet. Every piece of film was marked in order to keep the orientation constant during irradiation and read-out operations. Films were prepared and handled in dimmed light, wrapped in aluminium foil for storage and exposed to ambient light less than one minute during irradiation preparation. For the irradiation, the film was placed in a solid water phantom consisting of 12 plates of homogeneous water-equivalent RW3 material [35], measuring 30 × 30 × 1 cm^3 each.

Absolute dosimetry was performed for broad beams (BB) of 2 × 2 cm^2 size following as closely as possible the IAEA TRS 398 protocol [36] for low energy photons. The polychromatic X-ray irradiation spectrum used had a peak energy of 88 keV and a mean energy of 105 keV. This spectrum configuration of the ID17 biomedical beamline at the ESRF is used in pre-clinical experiments; the x-ray spectrum and a detailed discussion are presented in the work of Crosbie et al. [37]. Absolute dose measurement is performed placing an ionization chamber inside the water-equivalent phantom at the same position where films irradiation takes place; in this way, the energy spectrum reaching both detectors is the same and the energy variation of the spectrum along the propagation inside the phantom [38] does not affect the results. A calibrated PTW Pinpoint chamber TW31014 [39] in combination with a PTW electrometer (Webline) were used to measure the radiation dose at 2 cm depth from the surface of the RW3 phantom [9,15]. Following the absolute dosimetry procedure, five Gafchromic® films were irradiated for calibration in a limited dose range with BB doses of 60 Gy, 90 Gy, 100 Gy, 110 Gy and 140 Gy.

The irradiation with microbeams were defined starting from simulated output factor (OF) values. Nowadays, differences between dose simulation for MRT and experimental data vary up to 10% and further investigations are ongoing to reduce the gap. This complex problem is not addressed in this paper and previous simulated data were only used as indication for the microbeams irradiation. To match the delivered peak dose on the film around the centre of the established calibration curve, the irradiations were based on the OF values defined using Monte Carlo (MC) radiation transport simulations [40]. For the definition of the single microbeam irradiation, a couple of motorized slits were used to tune the desired beam width. Three films were irradiated with 25 μm, 50 μm and 75 μm wide beams.

Valley dose measurements were previously performed [13,15,27] and they present an important investigation since the absolute valley dose can be considered as the limiting factor for dose prescription in MRT [41]. Due to the big difference between peak and valley dose values within the same array of microbeams, the two quantities were evaluated separately, on two different films, because it was not possible to have both values within the defined calibration curve at the same time. For a peak dose value centred within the calibration curve, the valley dose value is too small to be properly measured. The delivered peak dose was therefore increased on the second film to match the valley dose value within the calibration curve. For an array of microbeams, the ratio between peak and valley dose, the so called PVDR value, can be simulated using MC [13] and it provides an estimate of the factor to be applied to increase the peak dose and bring the valley dose within the calibration curve.

For the valley dose evaluation, three films were exposed to an array of 50 μm wide microbeams spaced by a 400 μm pitch, and three field dimensions were used: 10 × 10 mm^2, 20 × 20 mm^2 and 30 × 30 mm^2. The overall horizontal extension of the radiation fields was defined by a couple of motorized slits. After the beam passes these slits it is split up by a multislit collimator (MSC) [42], i.e. a tungsten carbide block machined with 50 μm apertures that spatially fractionates the beam coming from the X-ray source. The minimum vertical extension of the microbeams was defined by a fixed aperture 500 μm high while the final height of the irradiated beam was obtained by vertically scanning the phantom in front of the synchrotron source. The combination of a motorized stage with a fast shutter specifically designed for MRT irradiation allows the definition of the beam height with sub-millimetric precision [43]. An example of a film irradiated with microbeams is reported in Fig. 1.

More recently, pencil beam irradiations have been performed with the purpose to increase healthy tissues tolerance, as compared to planar microbeams at identical peak doses, opening the possibility for whole brain radiotherapy [44]. Pencil beams are a few micrometre wide squared beamlets arranged into a two-dimensional array, resulting in higher PVDR. The realization of pencil beams is possible combining the use of two MSC to create the beam fractionation in both vertical and horizontal direction. This extreme configuration brings even more challenges in dosimetry at micrometric scale and so far, no experimental dose evaluation is present in literature. With the new dosimetry protocol based on the use of the OM, the dose analysis of pencil beams has become technically possible.

During previous in-vivo pre-clinical experiments [44], a whole mouse brain was irradiated with pencil beams and for dose verification, film dosimetry was performed. The films were positioned at 3 mm depth in a water equivalent phantom of similar size as a mouse head

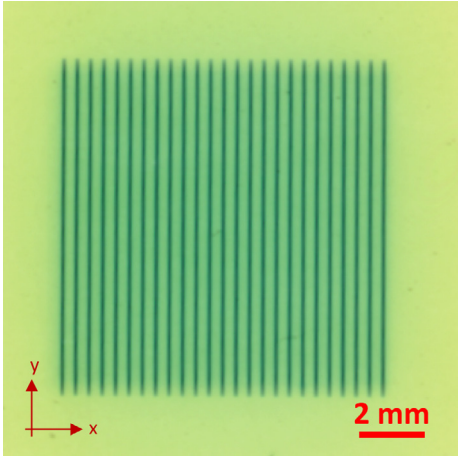

Fig. 1. HD-V2 film irradiated with an array of 50 μm wide microbeams spaced by a 400 μm pitch; the irradiated field is 1 × 1 cm^2. A reference coordinate system is defined.

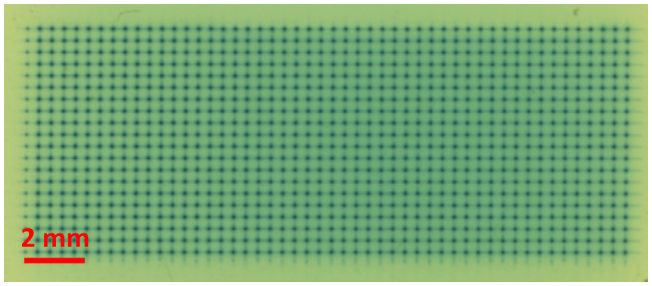

Fig. 2. Gafchromic® film irradiated with pencil beams.

and two films were irradiated separately adjusting the exposure time to have peak and valley dose values centred in the calibration curve, as done for microbeams irradiation. The same radiation field size used by Schültke et al. [44] was reproduced: a 20 mm wide and 8 mm high field of pencil beams with peaks of 50 × 50 μm^2 area, spaced by a 400 μm pitch. An example of a Gafchromic® film irradiated with pencil beams is reported in Fig. 2.

3.2. Read-out operation and calibration curves

The films were first analysed with the OM and then with the MDM since the microscope read-out is faster and causes less degradations to the films. Two metal masks with a central hole were pressing the film piece flat allowing for a focused image across the camera image. The use of glass slides is not recommended because the reflection of the light between the smooth polyester substrate of the HD-V2 film and the glass creates an interference pattern, known as Newton rings, visible in the acquired images that degrades the image quality. A picture of the setup is reported in Fig. 3.

The calibration curve was produced fitting the points with the equation suggested by D. Lewis [45]:

$$D(G) = a + b/(G - c)$$

where G is the grey value, $D(G)$ the corresponding dose and a, b, c are fitting parameters. This rational function fits properly the calibration points related to the film optical density measured by using transmitted or reflected light [46]. A non-irradiated film was included in the calibration curve because its intrinsic opacity was used to optimise the parameters of the OM avoiding saturation in the acquired images.

The MDM read-out requires a simplified method due to the limited stability of the instrument related to the mechanical drift of the optical components during read-out. It was not possible to identify the technical reason of this behaviour, but it was observed that the focus position of the instruments varies considerably after a few minutes. The value obtained from the same film analysed after 15 min without changing any parameter of the device setup can vary by up to 20%. For this reason, using the MDM, the calibration curve was reduced to four homogeneous films (60 Gy, 90 Gy, 100 Gy and 140 Gy) to decrease the time necessary for one read-out. To discriminate reliable measurements from erroneous ones, one of the BB films was read out twice, at the beginning and at the end of the series and measurements were only considered if the mean optical densities of the two scans show a difference of less than 1%.

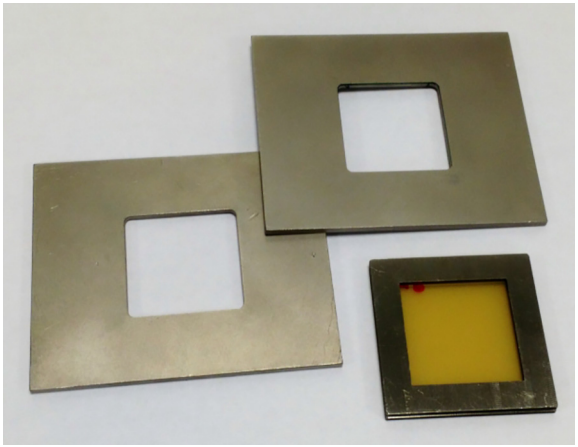

Fig. 3. Metal masks used for the film readout. In the bottom right corner, one piece of radiochromic film is held between two metal masks.

3.3. Image processing

The read-out procedure of the Gafchromic® films with the OM requires image processing including shading correction, correction of the CCD thermal noise and background light in the room. A white field image F was acquired without any sample loaded and a dark image B was acquired with the light source switched off. For each raw image of the film, the correction was performed in two steps: first, the raw image was corrected pixel-by-pixel by the camera noise (dark image $B(k,i)$):

$$I_b(k, i) = I_{raw}(k, i) - B(k, i)$$

where I_{raw} is the raw image and argument (k,i) denotes the pixel position. Second, the flat field correction (white field image, $F(k,i)$) was made dividing pixel-by-pixel the image $I_b(k,i)$ by the reference image $F(k,i)$ and multiplying the result by the average of the pixels in reference image $\overline{F(k, i)}$. It is possible to summarise the corrections of the defects by the formula below:

$$I_{fin}(k, i) = \frac{I_b(k, i)}{F(k, i)}\overline{F(k, i)}$$

For the films irradiated with BB, the grey value in the centre of the field was correlated with the measured dose of the PTW pinpoint chamber, which was also positioned in the centre of the field during the beam characterization. The dose delivered in the central 3 × 3 mm^2 area of the irradiated field was therefore considered for the creation of the calibration curve.

To align by eye the microbeams on the OM stage is not easy and a mistake of a few degrees affects the dose profile evaluation; therefore, the film image is digitally rotated. The precision in the selection of the microbeams angle from the digital image was checked by the evaluation of the dose profiles steepness for a range of angles around the selected one. Typically, the error made by the user is not more than ± 0.1 degree and this does not affect the dose evaluation.

As reported in the Materials section, the OM spatial resolution is higher compared to the film one and a dose analysis based on a single pixel value is not reasonable because of statistical uncertainties. For this reason, to reduce statistical uncertainties, the average over several pixels was used. For the evaluation of micro-planar beams, the resolution perpendicular to the microbeams (along the x-axis, Fig. 1) needs to be in the order of a few micrometres while parallel to the beam this condition can be relaxed. Consequently, the image was averaged over regions as high as the camera image (1040 pixels ≈ 1.3 mm) and 4 pixels in width equivalent to 5.16 μm. In the case of pencil beam irradiations, an average over a 25 × 25 pixel area was used to evaluate the peak dose and a region ~60 × 60 pixels, centred between four adjacent peaks, was selected for the valley dose evaluation.

The combined use of the motorized stage with the Zeiss software of the OM allows the quick acquisition of images up to 10 cm^2. However, digital elaboration is required because at the edges of the full image a clear loss of focus was visible with consequent invalidation of the dose analysis. This problem can be caused by a non-perfect alignment of the stage with the optics during the scan or by the presence of film bending when held by the stage. To solve this problem, a “multi-focus approach” was used: the entire area of interest was acquired several times changing each time the focus position. Subsequently, using post image

processing, the focused part of each image was selected and re-assembled into the final image.

3.4. Errors and uncertainties estimation related to the read-out procedure

In the definition of the measurement uncertainties related to the read-out procedure, the major contributions are given by the statistical noise linked to the microscopic inhomogeneities of the film and the intrinsic noise of the CCD camera [27]. For the OM read-out, the statistical noise was reduced by averaging over a number of pixels N, as described in the previous section. A smaller N value corresponds to a higher resolution but also to higher uncertainties.

The uncertainty was computed starting from the film images used for the definition of the calibration curve, linking the errors directly to the different dose values. They were divided into blocks Bi containing N pixels each and for every block Bi the mean of its pixels was calculated. In the ideal case, all blocks should have the same pixels mean value, but the defects of the film create differences. For this reason, the uncertainty for a specific dose was determined as the standard deviation of the mean value of the blocks B_i. The same approach was used for the evaluation of the MDM uncertainties where the standard deviation was calculated starting from the dose profile values of the films irradiated with BB. The uncertainties are the same for a defined dose for peak and valley because they are defined for every single point of the dose profile. Averaging over several peaks and valleys, and assuming they have the same dose value, this corresponds to an increase of the sampling area used for the evaluation; therefore, the statistical noise should decrease.

In addition, calibration errors due to the difference between experimental data and the fitted curve were considered. Finally, to quantify the reproducibility and reliability of the data acquired, all the films were analysed three times and the standard deviation of the values obtained from each film was evaluated and used as reproducibility indicator. One single read-out procedure starts with the OM/MDM setup, followed by the calibration curve definition and final evaluation of the film irradiated with microbeams. The reproducibility assessment does not include the uncertainty component relating to individual film variation, and additional components would be required to assess the overall uncertainty of the microbeam dose measured with film.

4. Results

4.1. Single microbeam evaluation

An example of the single microbeam peak dose profile obtained during one single acquisition with the two instruments, the MDM and the OM, is reported in Fig. 4. Each film is scanned three times with both instruments to obtain better statistics and the mean between the measurements was used for the analysis. Both instruments resulted in similar dose measurements for the peak dose, but the MDM profiles are more irregular than the dose profiles obtained with the OM. The resolution of the MDM is not sufficient to resolve microbeams less than 20 μm wide. In Fig. 4, the excess dose delivered to the right part of the beam is probably caused by reflection of photons at the inner surface of the collimating slit. Table 1 summarises the results of the measurements: each value corresponds to the average over three measurements and the differences between the measurements for both instruments are less than 3%.

The FWHM is evaluated for the three microbeams and the average value of the three measurements for each film is reported in table 2. The difference between the two instruments' results for FWHM values is around 2.5% for beams which are more than 50 μm wide, while it increases to around 10% for the thinner beams. The FWHM is systematically lower for the microscope.

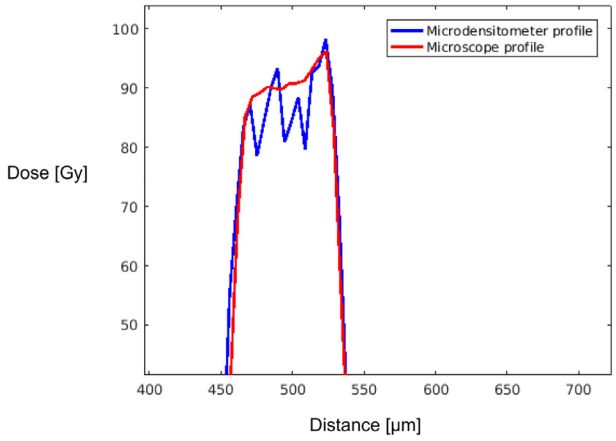

Fig. 4. Peak dose profile of one single microbeam of 75 μm width (FWHM) obtained with the microdensitometer (blue) and the microscope (red). (For interpretation of the references to colour in this figure legend, the reader is referred to the web version of this article.)

Table 1
Single microbeam dose evaluation.

DOSE	Microdensitometer	Microscope
Film 75 μm	91.9 ± 4.6 Gy	91.9 ± 3.2 Gy
Film 50 μm	96.3 ± 4.8 Gy	93.9 ± 3.3 Gy
Film 25 μm	103.9 ± 5.1 Gy	101.8 ± 3.1 Gy

Table 2
Single microbeam FWHM evaluation.

FWHM	Microdensitometer	Microscope
Film 75 μm	78.3 μm	77.4 μm
Film 50 μm	52.4 μm	51.6 μm
Film 25 μm	28.8 μm	25.8 μm

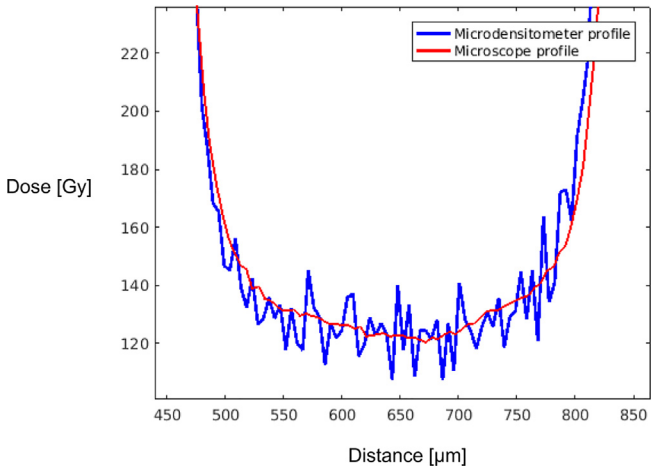

Fig. 5. Valley dose distribution profile obtained with the microdensitometer (blue) and the microscope (red). (For interpretation of the references to colour in this figure legend, the reader is referred to the web version of this article.)

4.2. Valley dose evaluation

In Fig. 5, an example of a single acquisition for valley profiles obtained with the two instruments is shown. The valley dose is measured in the centre of 1 × 1 cm^2, 2 × 2 cm^2 and 3 × 3 cm^2 field sizes with the analysis reported in table 3. Even if the profiles measured with the MDM are very noisy as compared to the profile measured with the OM,

Table 3
Valley dose measurement for a microbeams array; peak dose used is 6900 Gy for 1 × 1 cm^2 field, 3800 Gy for 2 × 2 cm^2 field and 2700 Gy for 3 × 3 cm^2 field.

Valley dose	Microdensitometer	Microscope
1 × 1 cm^2	131.9 ± 6.6 Gy	139.7 ± 4.1 Gy
2 × 2 cm^2	133.4 ± 6.7 Gy	134.3 ± 3.9 Gy
3 × 3 cm^2	121.4 ± 6.1 Gy	125.2 ± 3.7 Gy

Table 4
Microscope and microdensitometer uncertainties connected to the read-out. Uncertainties data not available for the MDM due to the lack of high-resolution capability have been marked with N/A.

Uncertainties	Microscope	Microdensitometer
Statistical noise		
20.0 × 2000.0 μm^2	0.5%–2.0%	8%–10%
5.2 × 1341.6 μm^2 (4 × 1040 pixels)	0.7%–2.5%	N/A
51.6 × 51.6 μm^2 (40 × 40 pixels)	3.0%–5.3%	N/A
25.8 × 25.8 μm^2 (20 × 20 pixels)	5.5%–7.5%	N/A
Calibration errors (between 60 and 140 Gy)	0.5%–2.5%	2%–8%
Reproducibility	0.4%–1.2%	3%–7%
Combined uncertainties		
20.0 × 2000.0 μm^2	2.5%–2.6%	8.8%–14.6%
5.2 × 1341.6 μm^2 (4 × 1040 pixels)	2.6%–3.0%	N/A
51.6 × 51.6 μm^2 (40 × 40 pixels)	3.9%–5.5%	N/A
25.8 × 25.8 μm^2 (20 × 20 pixels)	6.1%–7.7%	N/A

the results are comparable with dose differences being less than 5.5%.

4.3. Errors and uncertainties

The different components of errors and uncertainties are reported in table 4. The statistical noise was evaluated for each dose value of the calibration curve and regarding the OM, uncertainties were evaluated for the different resolutions used during the analysis while for the MDM, uncertainties were evaluated only for the best achievable resolution. Typically, the films irradiated with low dose present lower percentage errors compared to film irradiated with high dose. Calibration errors due to the difference between experimental data and the fitted curve are in the order of 1–1.5 Gy for OM calibration curves, while for the MDM are higher, 3–5 Gy.

The overall total uncertainty related to the read-out operation is estimated as square root of the sum of the squared contributions of statistical noise, calibration errors, and reproducibility. For the microscope, errors below 3.0% are possible for measurements performed averaging the dose on a 5 × 1300 μm^2 area. In the case of higher resolution, the uncertainty increases to around 6.1–7.7% for resolutions of 50 × 50 μm^2. For the MDM, the total error is usually between 8.8% and 14.6% with a resolution of 20 × 2000 μm^2. Regarding reproducibility and reliability, the variation between the final dose values for the OM is no more than 1.2%, while for the MDM is around 3–7%. For the total read-out uncertainty related to PVDR values, the statistical noise and reproducibility contribution must be considered twice because a separate read-out is necessary to obtain peak and valley dose values, while the calibration error need to be counted only once in case peak and valley dose are chosen to be the same for irradiation on two separate films.

4.4. Pencil beams

By using a microscope read-out, the experimental evaluation of pencil beams dose distributions was possible. In Fig. 6a and b, two digital images are shown, which are used for peak and valley dose evaluation respectively.

The peak dose is evaluated as average between the 12 peaks reported in Fig. 6a where areas of ≈35x35 μm^2 in the middle of the square peak fields are used and a dose of 111 ± 7 Gy is determined, with maximum standard deviation between the twelve measured peaks of 3.1%. The film for valley evaluation, reported in Fig. 6b, displays a pattern of vertical and horizontal lines connecting the individual pencil beams fields. Using the microscope read-out protocol, all the regions were evaluated separately. Unfortunately, in this case, the regions of the film along the line connecting the pencil beam areas received a too high dose, resulting in saturation of the film. For this reason, these parts of the film where not available for the analysis. Just the areas defined in the centre of four adjacent peaks were considered. In this case, the dose corresponds to the average obtained in a 75x75 μm^2 wide areas and it was determined to be 142 ± 5 Gy, with maximum standard deviation between the evaluated regions of 1.0%. The corresponding experimental PVDR at 3 mm depth for this configuration is 313.

5. Discussion

5.1. Materials discussion

Gafchromic® films are accurate high-resolution radiochromic detectors for MRT and are particularly practicable due to their

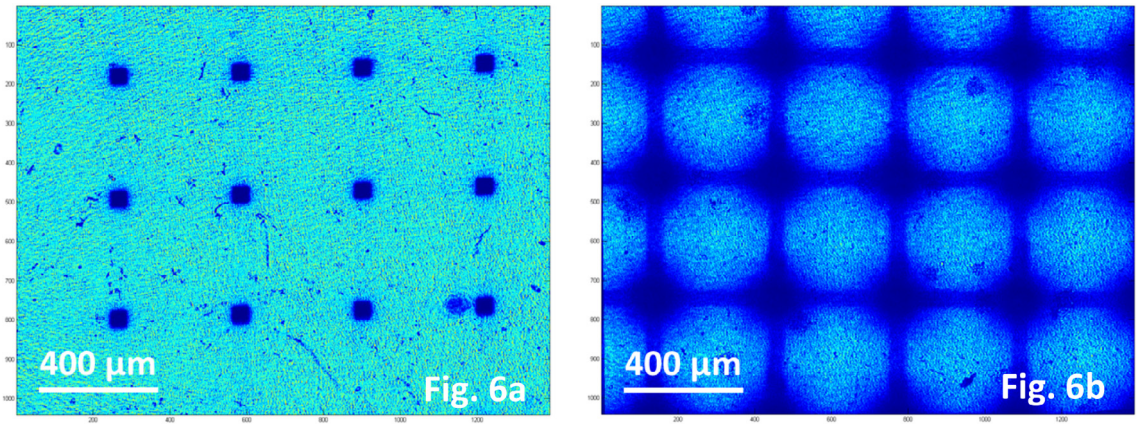

Fig. 6. (a) Digital microscope image of pencil beams for peak dose evaluation. (b) Microscope image of pencil beams irradiated with 65000 Gy in the peak; the mean valley dose between pencil beam is 142 Gy.

radiological tissue equivalence. They are widely used for benchmarking and quality assurance checks in pre-clinical research with their capability of visualizing the entire irradiated field at micrometric scale. In this work, HD-V2 Gafchromic® film were selected to be irradiated because they mainly differ from other type of radiochromic films, such as EBT3, in their dynamic dose range.

Irrespective of many drawbacks and technical difficulties, the MDM has been the only instrument available for film analysis in MRT for more than 15 years. However, the OM offers an easier to use read-out and it is simpler to manage compared to the MDM. For example, from past experience, independent observers have difficulties to agree on the focus point at the MDM, while the focus at the OM is easier to define because the film image is displayed live on a monitor.

Another important advantage in the use of the OM is the possibility to define a precise point of the field during the analysis, like the central point of the field, thanks to the combination of the CCD camera, the motorized stage and the Zeiss mosaiX software. With the MDM, the user can just align by eye the film under the optics, with a precision not better than some millimetres and this kind of error affects the measurements.

In addition, the resolution of the MDM along the direction perpendicular to the microbeams is really close to the dimension of the microbeams and in the other direction the best resolution is only 2 mm. Such low resolution is at the limit of usability for the dosimetry of microbeams and does not allow to evaluate the two-dimensional dose distribution of pencil beam fields. Here, we present an experimental measurement of a pencil beam dose distributions.

5.2. Methods discussion

Regarding the time necessary for the read-out of a series of films, there is a large difference between the two instruments, mainly due to their different mechanical stability. The MDM suffers from a drift of the focus position during the readout and it cannot be adjusted during the procedure, therefore the user is often forced to repeat the measurement. To obtain data from just one film irradiated with microbeams, hours of attempts are necessary. In addition, for each film irradiated with microbeams, the calibration film scans must be repeated because it is practically not possible to read out more than 5 or 6 films before mechanical drifts occur in the instrument. In contrast, using the microscope, all films need to be scanned only once. The image acquisition of the calibration films takes about 20 min, and 5 min are necessary for each film irradiated with microbeams.

The possibility to read out more films in less time using the OM allows to define a calibration curve with more points in the desired dose range or extend the dose range for the analysis. For the calibration curve of the MDM, no more than four films could be used for a 100 Gy wide dose range while with the OM a calibration curve over a 250 Gy range is possible with steps of 25 Gy. The limits of the microscope calibration curve range are connected to the dynamic range capability of the camera sensor, more specifically to the bright or dark sensitivity limits of the camera. Out of the defined dose range, saturation to the bright sensitivity limit of the camera occurs when trying to measure lower doses while the camera read-out is too noisy when trying to measure higher doses. Adjusting the LED voltage and the camera exposure time it is possible to select and shift the range of the calibration curve and an upper limit of the instrument for films irradiated with around 500 Gy was found.

The use of the OM digital camera provides 2-dimensional images and an image processing protocol has been developed to allow a versatile film analysis. The correction of the image artefacts is performed and the precise vertical alignment of the microbeams is digitally defined to remedy the non-precise manual placement of the films on the mechanical stage. At the end, the absence of a perfectly flat stage and/or sample surface is corrected by rearranging pieces of several image acquisitions with different focal points.

5.3. Results discussion

Despite the large technical and specification differences between the MDM and the microscope, the dose values obtained as average of three evaluations for each film differ no more than 4%. Even if the read-out with the two instruments seems to be quite equivalent, the maximum standard deviation between the measurements obtained with the MDM reaches 7% while values between 0.4% and 1.2% were obtained with the OM. The uncertainty estimation reveals that the microscope provides less error prone data compared to the MDM.

Working with the OM, a non-symmetric shape of the single microbeam irradiation was found when the single beam is defined by a pair of motorized slits which allow adjusting the gap according to the desired beam width. The presence of a higher dose at one edge of the beam, as visible in Fig. 4, is likely caused by a non-perfect parallel alignment of the slit, which leads to a reflection from the slit surface. This problem is not present using the multi slit collimator (MSC) to define the beams and a future project involving the design of a dedicated MSC for OF evaluation with single and fixed apertures of different widths is under development.

The read-out of the film irradiated in pencil beam configuration can be considered successful even if the uncertainties increase because of the high resolution used. Working in the pencil beam scenario the differences between simulated and experimental data increase: the simulation values obtained modelling the experimental set-up used and reported in previous work [44] present a PVDR value of 530, well above 313 evaluated with the films. Further investigation is required for pencil beams irradiation, starting from the presence of a dose grid visible in Fig. 6b. This grid is probably related to photon transmission in correspondence of the areas where only one of the two MSCs blocks the photons. Due to this “leakage”, the valley dose measured on the film increases, potentially explaining part of the difference in the PVDR values.

6. Conclusions

To determine the optical density at micrometric scale of radiochromic films irradiated with microbeams in the order of 50 μm wide, equivalent results with less read-out uncertainties are obtained using an OM instead of a MDM. The microscope allows more precise, accurate and reliable dose evaluation and it is a preferable and more versatile device able to overcome the limitations of the MDM. Using the OM, the 2-dimensional dose distribution of an irradiated film can be evaluated and the study of beams with cross section of $50 \times 50\ \mu m^2$ can be considered successful. The areas that can be analysed with the OM are considerably larger than with the MDM, allowing future implementation of film dosimetry protocols for the benchmark against dose simulations over the entire radiation field. These fundamental results in dosimetry for MRT clearly validate the transition from the previous protocol defined using the MDM to the one developed using the OM.

Declaration of Competing Interest

The authors declare not to have any conflict of interest.

Acknowledgment

This work was partially funded by the COST action TD1205 *Innovative methods in radiotherapy and radiosurgery using synchrotron radiation.*

References

[1] Laissue JA, Geiser G, Spanne PO, Dilmanian FA, Gebbers JO, Geiser M, et al. Neuropathology of ablation of rat gliosarcomas and contiguous brain tissues using a microplanar beam of synchrotron-wiggler-generated X rays. Int J Cancer

1998;78:654–60. https://doi.org/10.1002/(SICI)1097-0215(19981123)78:5<654::AID-IJC21>3.0.CO;2-L.
[2] Bräuer-Krisch E, Serduc R, Siegbahn EA, Le Duc G, Prezado Y, Bravin A, et al. Effects of pulsed, spatially fractionated, microscopic synchrotron X-ray beams on normal and tumoral brain tissue. Mutat Res – Rev Mutat Res 2010;704:160–6. https://doi.org/10.1016/j.mrrev.2009.12.003.
[3] Uyama A, Kondoh T, Nariyama N, Umetani K, Fukumoto M, Shinohara K, et al. A narrow microbeam is more effective for tumor growth suppression than a wide microbeam: an in vivo study using implanted human glioma cells. J Synchrotron Radiat 2011;18:671–8. https://doi.org/10.1107/s090904951101185x.
[4] Laissue JA, Blattmann H, Di Michiel M, Slatkin DN, Lyubimova N, Guzman R, et al. The weanling piglet cerebellum: a surrogate for tolerance to MRT (microbeam radiation therapy) in pediatric neuro-oncology. Penetrating Radiat Syst Appl III 2003;4508:65–73. https://doi.org/10.1117/12.450774.
[5] Bouchet A, Serduc R, Laissue JA, Djonov V. Effects of microbeam radiation therapy on normal and tumoral blood vessels. Phys Medica 2015;31:634–41. https://doi.org/10.1016/j.ejmp.2015.04.014.
[6] Laissue JA, Blattmann H, Wagner HP, Grotzer MA, Slatkin DN, Blattmann H, et al. Prospects for microbeam radiation therapy of brain tumours in children to reduce neurological sequelae. Dev Med Child Neurol 2007;49:577–81. https://doi.org/10.1111/j.1469-8749.2007.00577.x.
[7] Blattmann H, Gebbers JO, Bräuer-Krisch E, Bravin A, Le Duc G, Burkard W, et al. Applications of synchrotron X-rays to radiotherapy. Nucl Instruments Methods Phys Res Sect A Accel Spectrometers, Detect Assoc Equip 2005;548:17–22. https://doi.org/10.1016/j.nima.2005.03.060.
[8] Duke PJ. Synchrotron radiation: production and properties. Oxford University Press; 2009.
[9] Fournier P, Crosbie JC, Cornelius I, Berkvens P, Donzelli M, Clavel AH, et al. Absorbed dose-to-water protocol applied to synchrotron-generated x-rays at very high dose rates. Phys Med Biol 2016;61:N349–61. https://doi.org/10.1088/0031-9155/61/14/N349.
[10] Soellinger M, Rutz AK, Kozerke S, Boesiger P. 3D cine displacement-encoded MRI of pulsatile brain motion. Magn Reson Med 2009;61:153–62. https://doi.org/10.1002/mrm.21802.
[11] Donzelli M. Improving dose calculation and treatment planning techniques for microbeam radiation therapy with computational methods. Sutton, UK: ICR – Institute of Cancer Research; 2018.
[12] Manchado de Sola F, Vilches M, Prezado Y, Lallena AM. Impact of cardiosynchronous brain pulsations on Monte Carlo calculated doses for synchrotron micro- and minibeam radiation therapy. Med Phys 2018;45:3379–90. https://doi.org/10.1002/mp.12973.
[13] Martínez-Rovira I, Sempau J, Prezado Y. Development and commissioning of a Monte Carlo photon beam model for the forthcoming clinical trials in microbeam radiation therapy. Med Phys 2012;39:119–31. https://doi.org/10.1118/1.3665768.
[14] Bräuer-Krisch E, Rosenfeld A, Lerch M, Petasecca M, Akselrod M, Sykora J, et al. Potential high resolution dosimeters for MRT. AIP Conf Proc 2010;1266:89–97. https://doi.org/10.1063/1.3478205.
[15] Bräuer-Krisch E, Adam JF, Alagoz E, Bartzsch S, Crosbie J, DeWagter C, et al. Medical physics aspects of the synchrotron radiation therapies: Microbeam radiation therapy (MRT) and synchrotron stereotactic radiotherapy (SSRT). Phys Medica 2015;31:568–83. https://doi.org/10.1016/j.ejmp.2015.04.016.
[16] Doran SJ, Rahman ATA, Bräuer-Krisch E, Brochard T, Adamovics J, Nisbet A, et al. Establishing the suitability of quantitative optical CT microscopy of PRESAGE®radiochromic dosimeters for the verification of synchrotron microbeam therapy. Phys Med Biol 2013;58:6279–97. https://doi.org/10.1088/0031-9155/58/18/6279.
[17] McErlean CM, Bräuer-Krisch E, Adamovics J, Doran SJ. Assessment of optical CT as a future QA tool for synchrotron x-ray microbeam therapy. Phys Med Biol 2015;61:320–37. https://doi.org/10.1088/0031-9155/61/1/320.
[18] Fournier P, Cornelius I, Donzelli M, Requardt H, Nemoz C, Petasecca M, et al. X-Tream quality assurance in synchrotron X-ray microbeam radiation therapy. J Synchrotron Radiat 2016;23:1180–90. https://doi.org/10.1107/s1600577516009322.
[19] Livingstone J, Stevenson AW, Butler DJ, Häusermann D, Adam J-FF. Characterization of a synthetic single crystal diamond detector for dosimetry in spatially fractionated synchrotron x-ray fields. Med Phys 2016;43:4283–93. https://doi.org/10.1118/1.4953833.
[20] Archer J, Li E, Petasecca M, Dipuglia A, Cameron M, Stevenson A, et al. X-ray microbeam measurements with a high resolution scintillator fibre-optic dosimeter. Sci Rep 2017;7:12450. https://doi.org/10.1038/s41598-017-12697-6.
[21] Archer J, Li E, Petasecca M, Stevenson A, Livingstone J, Dipuglia A, et al. Synchrotron X-ray microbeam dosimetry with a 20 micrometre resolution scintillator fibre-optic dosimeter. J Synchrotron Radiat 2018;25:826–32. https://doi.org/10.1107/S1600577518003016.
[22] Mack A, Mack G, Weltz D, Scheib SG, Böttcher HD, Seifert V. High precision film dosimetry with GAFCHROMIC® films for quality assurance especially when using small fields. Med Phys 2003;30:2399–409. https://doi.org/10.1118/1.1593634.
[23] Devic S. Radiochromic film dosimetry: past, present, and future. Phys Medica 2011;27:122–34. https://doi.org/10.1016/J.EJMP.2010.10.001.
[24] Devic S, Tomic N, Lewis D. Reference radiochromic film dosimetry: review of technical aspects. Phys Medica 2016;32:541–56. https://doi.org/10.1016/j.ejmp.2016.02.008.
[25] Crosbie JC, Svalbe I, Midgley SM, Yagi N, Rogers PAW, Lewis RA. A method of dosimetry for synchrotron microbeam radiation therapy using radiochromic films of different sensitivity. Phys Med Biol 2008;53:6861–77. https://doi.org/10.1088/0031-9155/53/23/014.
[26] Nariyama N, Ohigashi T, Umetani K, Shinohara K, Tanaka H, Maruhashi A, et al. Spectromicroscopic film dosimetry for high-energy microbeam from synchrotron radiation. Appl Radiat Isot 2009;67:155–9. https://doi.org/10.1016/j.apradiso.2008.08.002.
[27] Bartzsch S, Lott J, Welsch K, Bräuer-Krisch E, Oelfke U. Micrometer-resolved film dosimetry using a microscope in microbeam radiation therapy. Med Phys 2015;42:4069–79. https://doi.org/10.1118/1.4922001.
[28] Ashland(R). Dosimetry media, type hd-v2. http://www.gafchromic.com/documents/gafchromic-hdv2.pdf. 2015.
[29] Cheung T, Butson MJ, Yu PKN. Post-irradiation colouration of Gafchromic EBT radiochromic film. Phys Med Biol 2005;50:N281–5. https://doi.org/10.1088/0031-9155/50/20/N04.
[30] Williams M, Metcalfe P. Radiochromic film dosimetry and its applications in radiotherapy. AIP Conf Proc 2011;1345:75–99. https://doi.org/10.1063/1.3576160.
[31] Butson MJ, Yu PKN, Cheung T, Metcalfe P. Radiochromic film for medical radiation dosimetry. Mater Sci Eng R Reports 2003;41:61–120. https://doi.org/10.1016/S0927-796X(03)00034-2.
[32] Morri M. Experimental dosimetry of high dose rates X-ray microbeams fields for the. MRT 2010.
[33] Imaging DF. Microscopy from Carl Zeiss AxioCam MRm from Carl Zeiss – More Information at Low Light Intensities. 2015.
[34] Niroomand-Rad A, Chiu-Tsao ST, Soares CG, Meigooni AS, Kirov AS. Comparison of uniformity of dose response of double layer radiochromic films (MD-55-2) measured at 5 institutions. Phys Medica 2005;21:15–21. https://doi.org/10.1016/S1120-1797(05)80015-8.
[35] PTW. Radiation Medicine Qa. Health Phys 2016:98. http://www.ptw.de/acrylic_and_rw3_slab_phantoms0.html.
[36] Musolino SV. Absorbed Dose Determination in External Beam Radiotherapy: An International Code of Practice for Dosimetry Based on Standards of Absorbed Dose to Water; Technical Reports Series No. 398, vol. 81. 2001. doi:10.1097/00004032-200111000-00017.
[37] Crosbie JC, Fournier P, Bartzsch S, Donzelli M, Cornelius I, Stevenson AW, et al. Energy spectra considerations for synchrotron radiotherapy trials on the ID17 biomedical beamline at the European Synchrotron Radiation Facility. J Synchrotron Radiat 2015;22:1035–41. https://doi.org/10.1107/s1600577515008115.
[38] Tomic N, Papaconstadopoulos P, Bekerat H, Antunovic G, Aldelaijan S, Seuntjens J, et al. Monte Carlo simulations of different CT X-ray energy spectra within CTDI phantom and the influence of its changes on radiochromic film measurements. Phys Medica 2019;62:105–10. https://doi.org/10.1016/j.ejmp.2019.04.015.
[39] PTW. Ionizing Radiation, Detectors. 2016.
[40] Clavel A. Microdosimetrie dans le cadre des assais precliniques de la radiotherapie a microfausceaux. 2012.
[41] Smyth LML, Senthi S, Crosbie JC, Rogers PAW. The normal tissue effects of microbeam radiotherapy: What do we know, and what do we need to know to plan a human clinical trial? Int J Radiat Biol 2016;92:302–11. https://doi.org/10.3109/09553002.2016.1154217.
[42] Bräuer-Krisch E, Bravin A, Zhang L, Siegbahn E, Stepanek J, Blattmann H, et al. Characterization of a tungsten/gas multislit collimator for microbeam radiation therapy at the European Synchrotron Radiation Facility. Rev Sci Instrum 2005;76.. https://doi.org/10.1063/1.1915270.
[43] Renier M, Brochard T, Nemoz C. Thomlinson W. A white-beam fast-shutter for microbeam radiation therapy at the ESRF. Nucl Instruments Methods Phys Res Sect A Accel Spectrometers, Detect Assoc Equip 2002. https://doi.org/10.1016/S0168-9002(01)00905-6.
[44] Schültke E, Trippel M, Bräuer-Krisch E, Renier M, Bartzsch S, Requardt H, et al. Pencilbeam Irradiation technique for whole brain radiotherapy: technical and biological challenges in a small animal model. PLoS ONE 2013;8:1–9. https://doi.org/10.1371/journal.pone.0054960.
[45] Micke A, Lewis D. yu X. SU-E-I- 63: multi-channel film dosimetry with non-uniformity correction. Med Phys 2011;38:3410. https://doi.org/10.1118/1.3611636.
[46] Aldelaijan S, Devic S. Comparison of dose response functions for EBT3 model GafChromic™ film dosimetry system. Phys Medica 2018. https://doi.org/10.1016/j.ejmp.2018.05.014.